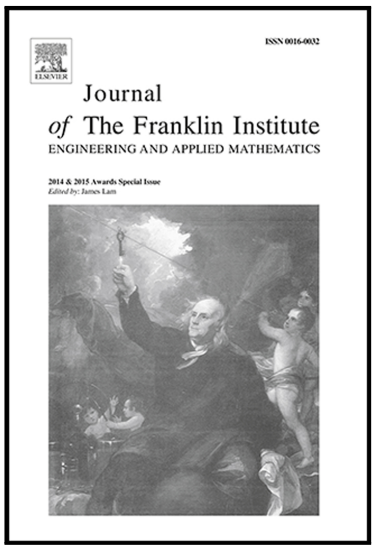

Rotary inverted pendulum with magnetically external perturbations as a source of the pendulum's base navigation commands

Gisela Pujol-Vazquez, Leonardo Acho, Saleh Mobayen,
Amelia Nápoles, Vega Pérez

PII: S0016-0032(18)30215-1
DOI: 10.1016/j.jfranklin.2018.03.013
Reference: FI 3385

To appear in: *Journal of the Franklin Institute*

Received date: 27 February 2017
Revised date: 26 February 2018
Accepted date: 13 March 2018

Please cite this article as: Gisela Pujol-Vazquez, Leonardo Acho, Saleh Mobayen, Amelia Nápoles, Vega Pérez, Rotary inverted pendulum with magnetically external perturbations as a source of the pendulum's base navigation commands, *Journal of the Franklin Institute* (2018), doi: 10.1016/j.jfranklin.2018.03.013

Rotary inverted pendulum with magnetically external perturbations as a source of the pendulum's base navigation commands

Gisela Pujol-Vazquez[a,*], Leonardo Acho[b], Saleh Mobayen[c], Amelia Nápoles[d], Vega Pérez[e]

[a] *Department of Mathematics, Universitat Politècnica de Catalunya-BarcelonaTech (ESEIAAT), Terrasa, Spain.*
[b] *Department of Mathematics, Universitat Politècnica de Catalunya-BarcelonaTech (EEBE), Barcelona, Spain.*
[c] *Department of Electrical Engineering, University of Zanjan, Zanjan, Iran.*
[d] *Department of Mechanical Engineering, Universitat Politècnica de Catalunya-BarcelonaTech (EPSEVG), Vilanova, Spain.*
[e] *Department of Strength of Materials and Structural Engineering, Universitat Politècnica de Catalunya-BarcelonaTech (EEBE), Barcelona, Spain.*

Abstract

The main objective of this paper is to drive a rotary inverted pendulum by following a desired navigation instruction. This navigation is commanded by the user through a new electromagnetic device which is allowed to perturb the pendulum from its upright position. This apparatus consists of an electronic magnetic driving circuit to introduce commands and realized via two operated magnetic coils. So, the external programmed magnetic perturbation can be seen as external commandments. Therefore, the control problem statement is solved via a modified regulation control implementation, to maintain the pendulum on its upright position and giving free manipulation of the base of the rotary inverted pendulum. Hence, by using the corresponding H_∞-linear matrix inequality technique, a static state controller is designed and tested experimentally so supporting our findings.

Keywords: Rotary inverted pendulum; H_∞-linear matrix inequality technique; Control theory; Electromagnetic manipulator; External perturbations.

*Corresponding author: Colom 1, 08222 Terrassa, Spain. (email: gisela.pujol@upc.edu).

1. Introduction

A rotary inverted pendulum, also named Furuta pendulum, is usually employed as a benchmark case study to investigate various control techniques due to its inherent instability and intrinsic nonlinearities (see [1]-[3] and references there in). As an under-actuated nonlinear dynamical system, it has more degrees-of-freedom than control inputs. Under-actuated systems have important engineering challenges and applications such as free-flying space robots [4], underwater robots [5], manipulators with structural flexibility [6], chaotic systems [7], sliding mode control [8], spacecraft systems [9]-[10], underactuated humanoids robots [11], switched control [12], etc. In particular, the inverted pendulum is related to missile guidance, where the thrust is actuated at the bottom of a tall vehicle [13]. Control and stabilization of these systems are challenging tasks and are topics of research for both engineers and applied mathematicians. Moreover, a personal transporter vehicle, called Segway (wheeled inverted pendulum system) is also based on the stabilization principle of inverted pendulum system [14]-[16]. On the other hand, the rotary inverted pendulum has been a well-known academic system to analysis and design a great variety of controllers, bracing from the classical to the advanced non-linear ones [17]-[24]. In [25], the authors design a robust control approach for the rotary inverted double pendulum, where the regulated signal does not depend on the control input as our control design does. Almost all of them are designed to fulfill the regulation and tracking control objectives, being robust against external perturbations [26]-[32]. The usual theory to solve a tracking problem is based on reducing the error between the actual position and the desired trajectory (see [30]-[36] and references in it). In these papers, a variety of control strategies are presented: composite controller, velocity-tracking controller, fuzzy control, adaptive control, terminal sliding mode control, etc.

The motivation of this paper is to grant an experimental platform to navigate an

under-actuated system by external perturbations. Hence, the proposed methodology is based on inducing a magnetic perturbation manipulated by the user. Moreover, and from the control objective point of view, it is necessary to adequate the dynamic model of the system to use this perturbation as a healthy agent to navigate the system. The new control aim is motivated by the remote control of inverted pendulum [37]-[39]. Usually, position commands are given by some elements (network or wireless system) through input channel. However, in the present paper, none desired trajectory is introduced in the system. The desired position is introduced via the compensation of the external perturbation. Then, the 'tracking' problem is solved as a regulation perturbed method.

To the best of our knowledge, the tracking control purpose of the inverted pendulum via external perturbations without contact has not been previously proposed. In references [40]-[41], the authors use tiny perturbations on the system parameters to stabilize the chaotic dynamic behaviors, and to direct trajectories to a desired state. In the present paper, the system is not perturbed parametrically, and the external forces are added to perturb the dynamic behavior. Therefore, by using the H_∞-linear matrix inequality (LMI) technique [42]-[45], a robust control method is provided. It is important to note that we are using standard theory applied on our novel platform experiment. Hence, to drive the base of the rotary inverted pendulum, we use external perturbations magnetically produced.Thus, an electronic Magnetic Driving Commands (MDC) device is here developed by using two coils and implemented onto the inverted pendulum to magnetically disturb it (see Figure 1). This kind of device which appears in engineering topics is motivated by the fact to manipulate an object without touching it. In our realization, these coils create magnetic field forces that *slightly* attract (perturb) the pendulum to the left or right, depending on the corresponding activated user command switches located in MDC device. This perturbation is then *compensated* by designed H_∞-LMI-based controller producing angular displacement on the base of the pendulum, keeping its upright position. In this way, the designed system is *navigated* at

the disposal of the user command. Therefore, the external disturbance induces a desired movement (clockwise and counter-clock wise) on the rotary inverted pendulum mechanical support. This may be a novel experiment to impact academic teaching on external control design of underactuated mechanical systems. Obviously, to fulfill this control objective, the control problem statement and modeling require to be correctly modified.

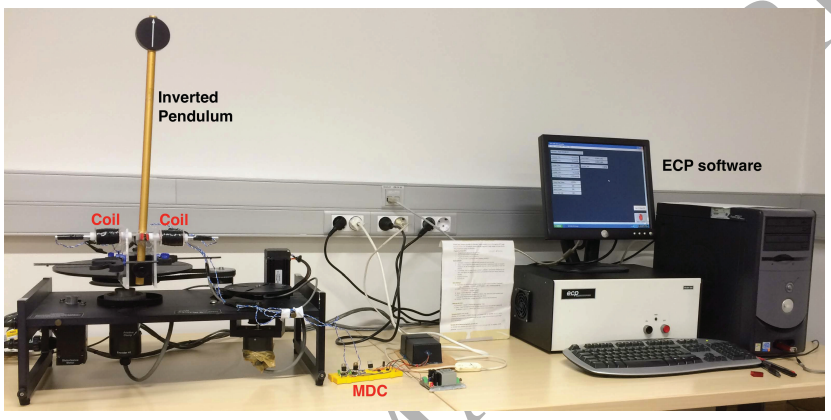

Figure 1: Our experimental platform composed by a computer with the Educational Control Products (ECP) software in it ([46]); the rotary inverted pendulum; the MDC-device and the coils. Note that the pendulum is attached to the load disk.

2. Problem statement

The principal aim of this paper is to obtain a new electromagnetic device able to reproduce the navigation of a mechanical system without touching it. This navigation is obtained because the controller tries to stabilize the system, when commanded disturbance appears. Then, designing a robust control law, the system maintains this navigation despite external disturbances and parametric uncertainties. The control design does not depend directly on a desired trajectory, because the system detects it as an external perturbation.

More precisely, two objectives have been stated. One is to design and implement an electromagnetic device to produce external magnetic disturbance

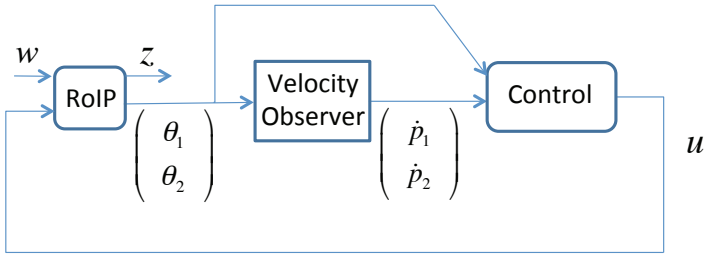

Figure 2: Schematic diagram of the rotary inverted pendulum (RoIP): w is the external perturbation produced by the MDC; $[\theta_1, \theta_2]^T$ is the measurable output; z is the virtual output to be compared to w [42]; $[\dot{p}_1, \dot{p}_2]^T$ is the observed velocity vector; u is the control input.

forces onto the rotary inverted pendulum. So, this device is used to perturb the system. Then, the proposed controller maintains the pendulum on its upright position by obtaining the desired system navigation. Thence, we drive the pendulum by following an induced commanded-by-the-user trajectory through this magnetic device, which allows to perturb the pendulum from its upright position. Finally, the second objective consists of design a new regulation control algorithm. That is, to solve the perturbed regulation control problem, a state-feedback LMI-robust controller is designed, to stabilize the Furuta's pendulum on its upright position. A design condition is imposed: the feedback controller needs to release the load disk position in order to be externally manipulated. Hence, the pendulum is stabilized for any value of the angular position of load disk. Furthermore, only two variables are available: pendulum and load disk angular positions. Then, observers are constructed to obtain the velocities of the pendulum and load disk (see Figure 2).

3. Rotary inverted pendulum model

This section presents the mechanical description of the rotary inverted pendulum and its mathematical model according to the academic experimental platform M220 reported in [46]. The rotating base system is driven by a DC-motor (see Figure 3) where the inverted pendulum is attached. The angular-rotation

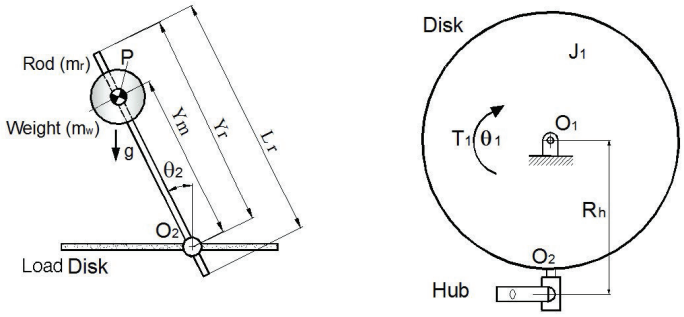

Figure 3: Mechanical diagram representation of rotary inverted pendulum [46].

position of the base (the load disk mechanical system) with respect to O_1 is represented by $\theta_1(t)$, and $\theta_2(t)$ is the angular-rotation position of the pendulum with respect to O_2. For simplicity, in our models, the dependence on variable time t is omitted. On the other hand, Figure 3 and data in Table 1 describe the parameters of the rotary pendulum system, where the subscripts r and w refer to the pendulum rod and weight, respectively; and the parameters L and R refer to the length and radius of the respective cylinders, correspondingly.

To obtain a mathematical model of the rotary inverted pendulum, the following assumptions are made:

1. The system starts near to its non-stable equilibrium point;
2. The pendulum does not move far away from this non-stable equilibrium point;
3. A small perturbation can be tolerated by our control system.

3.1. Euler-Lagrange's equations

The motion equations for the rotary inverted pendulum around unstable equilibrium point are here obtained by using Lagrange's theory, which leads to a second-order under-actuated model. By examining Figure 3, the total kinetic energy of the system $K_c = K_1 + K_2 + K_3$, where K_1 is the kinetic energy of the disk rotation; K_2 of the pendulum mass center transfer; and K_3 of the pendulum

Table 1: Parameters of rotary inverted pendulum and load disk [46].

Parameter	Description
m_r, m_w	Masses of the rod and attached weight (kg).
m	Total mass of the pendulum: $m = m_r + m_w$.
P	Position of the additional mass (m).
Y_m, Y_r	Pendulum and P length to the attach load point (m).
L_r	Length of the pendulum (m).
O_2	Position of the pendulum attached to the load disk (m).
θ_1	Angular position of the disk with respect to O_1 (rad).
θ_2	Angular position of the pendulum with respect to O_2 (rad).
J_1	Moment of inertia of all elements that move uniformly with the base disk $(kg \cdot m^2)$.
R_h	Distance between O_1 and O_2 (m).
R_w	Weight radius (m).
T_1	Rotation torque generated by the load disk (N/rad).
O_1	Center of the base disk.
J_x, J_y, J_z	Pendulum inertia tensions, relative to its center of mass $(kg \cdot m^2)$.
l_{cg}	Center of gravity of the combined pendulum rod and weight (m).
c_1	Viscous friction coefficient.
g	Gravity constant $(m \cdot s^{-2})$.

rotation relative to the pendulum mass center, are [46]:

$$K_1 = \frac{1}{2} J_1 \dot{\theta}_1^2, \tag{1}$$

$$K_2 = \frac{1}{2} m \left(\left(\dot{\theta}_1 R_h + \dot{\theta}_2 l_{cg} \cos(\theta_2) \right)^2 + \left(\dot{\theta}_2 l_{cg} \sin(\theta_2) \right)^2 + \right.$$
$$\left. + \left(\dot{\theta}_1 l_{cg} \sin(\theta_2) \right)^2 \right), \tag{2}$$

$$K_3 = \frac{1}{2} J_z \dot{\theta}_2^2 + \frac{1}{2} J_x \left(\dot{\theta}_1 \sin(\theta_2) \right)^2 + \frac{1}{2} J_y \left(\dot{\theta}_1 \cos(\theta_2) \right)^2, \tag{3}$$

where $l_{cg} = \frac{m_r(y_r - \frac{1}{2}L_r) + m_w y_m}{m_r + m_w}$ is the center of gravity of the combined pendulum rod and weight. The terms J_x, J_y and J_z are the moments of inertia for the pendulum (x-perpendicular to z and y; y - along the rod; z - along the rotation axis), relative to its center of mass given by:

$$\begin{aligned} J_x &= \frac{1}{12}m_r L_r^2 + \frac{1}{4}m_w R_w^2, \\ J_y &= \frac{1}{4}m_w R_w^2, \\ J_z &= \frac{1}{12}m_r L_r^2 + \frac{1}{2}m_w R_w^2. \end{aligned}$$

Usually the parameters L_w (weight length) and R_r (pendulum rod radius) are very small in relation to other terms which can be neglected in the above expressions. On the other hand, the corresponding potential energy is:

$$U = mgl_{cg}\cos(\theta_2). \tag{4}$$

By using the Lagrange function $L = K_c - U$, we obtain the equations of motion as:

$$\frac{d}{dt}\left(\frac{\partial L}{\partial \dot{\theta}_i}\right) - \frac{\partial L}{\partial \theta_i} = T_i \ , \ i = 1, 2, \tag{5}$$

where T_i, $i = 1, 2$, are virtual forces ($T_2 = 0$). From (5), and taking into account the viscous friction c_1 at the load disk, for $i = 1$ we arrive to:

$$\begin{aligned} \ddot{\theta}_1\left(\bar{J}_1 + \bar{J}_x\sin^2(\theta_2) + J_y\cos^2(\theta_2)\right) - \dot{\theta}_2^2 m R_h l_{cg}\sin(\theta_2) + c_1\dot{\theta}_1 + \\ + \ddot{\theta}_2 m R_h l_{cg}\cos(\theta_2) + \dot{\theta}_1\dot{\theta}_2(\bar{J}_x - J_y)\sin(2\theta_2) = \quad T_1. \end{aligned} \tag{6}$$

Finally, for $i = 2$ in (5), the second equation of motion is:

$$\begin{aligned} \ddot{\theta}_1 m R_h l_{cg}\cos(\theta_2) + \ddot{\theta}_2\bar{J}_z - \tfrac{1}{2}\dot{\theta}_1^2(\bar{J}_x - J_y)\sin(2\theta_2) - mgl_{cg}\sin(\theta_2) + \\ mR_h\sin(\theta_2)\dot{\theta}_1 - \dot{\theta}_1\dot{\theta}_2 m R_h l_{cg}\sin(\theta_2) = \quad 0, \end{aligned} \tag{7}$$

where

$$\begin{aligned} \bar{J}_1 &= J_1 + mR_h^2, \\ \bar{J}_x &= J_x + ml_{cg}^2, \\ \bar{J}_z &= J_z + ml_{cg}^2 \ . \end{aligned}$$

Note: Friction on the mechanical pendulum system can be neglected. Actually, the ECP manufacturer also specifies this assessment [46]. However, Appendix 9.1 explains that if friction is considerable, it can be viewed as a perturbation.

4. Robust control design

Following our previous problem statement, we consider a reduced model with $\mathbf{x} = [\dot{\theta}_1, \theta_2, \dot{\theta}_2]$. The equilibrium point is $\mathbf{x}^* = [0, 0, 0]^T$. For the control design, we use a linear model of the system and a robust H_∞ control theory, to be solved via LMI tools [45], [47].

4.1. Linear model

Considering the rotating base system in inverted situation, equations (6)-(7) may be linearized around the upright position $\theta_1 = 0$ and $\theta_2 = 0$, yielding:

$$\ddot{\theta}_1(\bar{J}_1 + J_y) + \ddot{\theta}_2 m R_h l_{cg} + c_1\dot{\theta}_1 = T_1,$$

$$\ddot{\theta}_1 m R_h l_{cg} + \ddot{\theta}_2 \bar{J}_z - m g l_{cg}\theta_2 = 0.$$

These equations may be rewritten as:

$$\ddot{\theta}_1 = \frac{1}{p}\left(-c_1\bar{J}_z\dot{\theta}_1 - m^2 l_{cg}^2 R_h g\,\theta_2 + \bar{J}_z T_1\right), \tag{8}$$

$$\ddot{\theta}_2 = \frac{1}{p}\left(m R_h l_{cg} c_1\dot{\theta}_1 + m g l_{cg}(\bar{J}_1 + J_y)\theta_2 - m R_h l_{cg} T_1\right), \tag{9}$$

where $p = \bar{J}_z(\bar{J}_1 + J_y) - (m R_h l_{cg})^2$. Introducing external $\mathcal{L}_2$ perturbation w by modifying the pendulum angular position, θ_2 is modified as $\theta_2 + w$. If w is not constant, we have to consider the perturbation as $\omega = [w, \dot{w}]$, with the assumption that $\dot{w} \in \mathcal{L}_2$. Defining $\mathbf{x} = [\dot{\theta}_1, \theta_2, \dot{\theta}_2]$, the matrix representation of the linear rotary inverted pendulum model (8) and (9) is

$$\dot{\mathbf{x}} = \mathbf{A}\mathbf{x} + \mathbf{B_2}u + \mathbf{B_1}\omega, \tag{10}$$

where $u = T_1$ is the control effort, and

$$\mathbf{A} = \begin{bmatrix} \frac{-\bar{J}_z c_1}{p} & \frac{-m^2 l_{cg}^2 R_h g}{p} & 0 \\ 0 & 0 & 1 \\ \frac{m R_h l_{cg} c_1}{p} & \frac{m g l_{cg}(\bar{J}_1 + J_y)}{p} & 0 \end{bmatrix},$$

$$\mathbf{B_1} = \begin{bmatrix} \frac{-m^2 l_{cg}^2 R_h g}{p} & 0 \\ 0 & 1 \\ \frac{m g l_{cg}(\bar{J}_1 + J_y)}{p} & 0 \end{bmatrix}, \quad \mathbf{B_2} = \begin{bmatrix} \frac{\bar{J}_z}{p} \\ 0 \\ \frac{-m l_{cg} R_h}{p} \end{bmatrix}.$$

4.2. LMI control design

In most control designs, a controller is sought not only to stabilize the system, but also to ensure some satisfactory degree of performance in front of perturbations. The H_∞ control theory deals with this problem, obtaining an upper bound of the H_∞ norm [42]-[48]. In [42], the H_∞ problem is established via the resolution of Riccati inequalities. The common tricks used to turn it into LMIs are the Projection lemma's and the Schur complements [43]-[48]. Since then, the use of LMI has a wide range of applications (networked systems [49], fuzzy control [50], circuit control [51], etc).

A linear state-feedback strategy is adopted to design the robust control defined by $u = \mathbf{Kx}$ (see Fig. 2). Then, the gain matrix $\mathbf{K}$ is obtained from H_∞ theory [42]. This theory is based on reducing the effect of an external disturbance ω on a virtual variable $\mathbf{z}$, defined by the user. In our case, $\mathbf{z}$ is defined to control the contribution of the perturbation on all the state variables of the reduced model, with special focus on the control effort u. Hence, we have

$$\mathbf{z} = [\dot{\theta}_1, \theta_2, \dot{\theta}_2, u]^T = \mathbf{C_1 x} + \mathbf{D_{12}} u, \tag{11}$$

where

$$\mathbf{C_1} = \begin{bmatrix} 0.1 & 0 & 0 \\ 0 & 0.1 & 0 \\ 0 & 0 & 0.1 \\ 0 & 0 & 0 \end{bmatrix}, \ \mathbf{D_{12}} = [0 \ 0 \ 0 \ 1]^T.$$

The values of $\mathbf{C_1}$ and $\mathbf{D_{12}}$ are established to emphasize the effect of the disturbance on the robust control law u. A practical way to solve this problem is to consider a Lyapunov function $V(\mathbf{x})$ such that for any nonzero $\mathbf{x}$ and input $\omega \in \mathcal{L}_2$, the following condition holds ([52]):

$$\frac{d}{dt}V(\mathbf{x}) + \gamma^{-1} \ \mathbf{z}^T\mathbf{z} - \gamma \ \omega^T\omega < 0. \tag{12}$$

Then, an H_∞ performance bound γ for the closed-loop system (10)–(11) with $u = \mathbf{Kx}$ is ensured.

Definition 1 (H_∞ Control [52]). *If there exists a matrix* $\mathbf{K}$ *such that (12) holds, the control law* $u = \mathbf{Kx}$ *is said to be an* H_∞ *controller for the system (10)–(11).*

That is, the system is internally stable (the closed-loop system is asymptotically stable if $\omega = 0$), with H_∞ norm less than γ, i.e., $\|\mathbf{z}\|_\infty \leq \gamma^2\|\omega\|_\infty$ for $\omega \in \mathcal{L}_2$. To simplify the notation, in symmetric block matrices or long matrix expressions, symbol $*$ is used as an ellipsis for terms that are induced by symmetry.

Theorem 1 ([47, 53]). *Consider the system (10)-(11). If there exist* $\gamma > 0$, *matrices* $\mathbf{N}$, $\mathbf{Y} > 0$ *symmetric and* $\mathbf{V}$ *regular such that the LMI*

$$\begin{bmatrix} -(\mathbf{V}^T + \mathbf{V}) & * & * & * & * & * \\ \mathbf{AV} + \mathbf{Y} + \mathbf{B}_2\mathbf{N} & -\mathbf{Y} & * & * & * & * \\ 0 & \mathbf{B}_1^T & -\gamma & * & * & * \\ \mathbf{C}_1\mathbf{V} & 0 & 0 & -\gamma & * & * \\ \mathbf{N} & 0 & 0 & 0 & -\gamma & * \\ \mathbf{V} & 0 & 0 & 0 & 0 & -\mathbf{Y} \end{bmatrix} < 0, \tag{13}$$

is feasible, then u is an H_∞ controller defined by:

$$u = \mathbf{N}\mathbf{V}^{-1}\,\mathbf{x}. \tag{14}$$

The proof of Theorem 1 is presented is Appendix 9.2.

5. Experiments to an industrial emulator

The purpose of this section is to test the behavior of the new MDC device, and also to study the effectiveness of the obtained control law (14). Then, experiments are performed on an ECP Model 220 industrial emulator with inverted pendulum, that includes a PC-based platform and DC brushless servo-system [46]. The mechatronic system includes a motor used as servo actuator, a power amplifier and two encoders which provide accurate position measurements; i.e., 4000 lines per revolution with $4X$ hardware interpolation giving 16000 counts per revolution to each encoder; 1 count (equivalent to 0.000392 radians or 0.0225 degrees) is the lowest angular measurable [46]. Previously evaluated control law (15) may be used directly for control modeling, scaled by appropriate system gains (amplifier and software gains and motor torque constants). The inverted pendulum is modified attaching an external electromagnetic commanded disturbance device, introducing uncertainties on the parameters values of the experiment. That is, we consider the nominal values presented in Table 2 [46]. It is well-known that a real experiment always contains uncertainties on its parameters. Moreover, in the present experiment, a device is attached to the load disk, modifying the mass of the system (see Fig. 4). In order to study the robustness of the proposed controller, the system parameters are not adjusted. Despite of it, the H_∞-LMI control (15) shows an acceptable behavior. Also, a disturbance observer is implemented to confirm that the navigation of the system is due to the external perturbation.

5.1. Magnetic Driving Command (MDC)

An MDC is implemented into the inverted pendulum to perturb it, creating a magnetic field that attracts the pendulum to the left or right (commanded

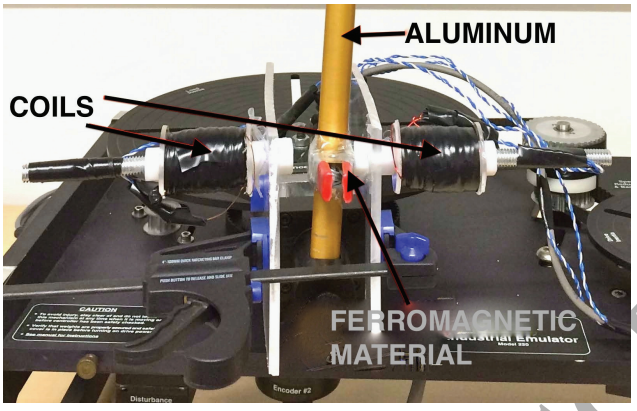

Figure 4: MDC device. The pendulum arm is made of aluminum, so a ferromagnetic device has to be attached. The coils induce the electromagnetic field forces.

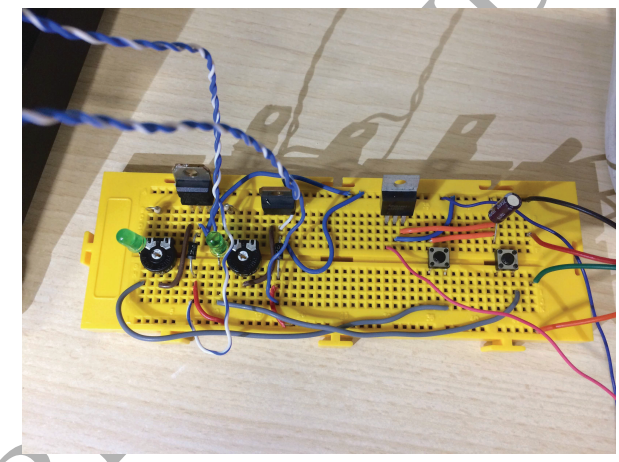

Figure 5: Electronic implementation of the MDC device.

by the user). This perturbation is detected by the platform, and the controller stabilizes it by an angular displacement of the load disk. So, the external disturbance induces a desired movement (clockwise and anticlockwise) on the platform. See Figures 4, 5 and 6. During the experiments, it is important to note that the pendulum rod does not contact with the magnetos (see the video uploaded with the main paper).

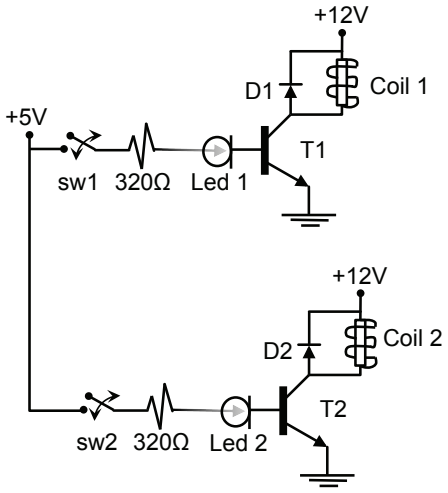

Figure 6: MDC's electronic circuit. SW1 and SW2 are the user commanded switches that activate the corresponding coil to perturb the inverted pendulum. The other electronic elements are the basic ones.

Table 2: Parameter values of rotary pendulum and load disk [46].

m_r	$0.039\,kg$	J_1	$0.003\,kg\,m^2$
m_w	$0.018\,kg$	R_h	$0.194\,m$
y_m	$0.39\,m$	R_w	$0.025\,m$
y_r	$0.43\,m$	c_1	$3.5\,10^{-3}\,N\,ms$
L_r	$0.47\,m$	g	$9.8\,m\,s^{-2}$

5.2. Experimental results

Table 2 presents the parameters values of the rotary inverted pendulum [46]. It is important to note that these values do not take into account the mass and position of the MDC device, introducing some model uncertainties. Then, from Table 2, the system equations (10)-(11) become:

$$\mathbf{A} = \begin{bmatrix} -1.1379 & -28.769 & 0 \\ 0 & 0 & 1 \\ 0.7219 & 50.229 & 0 \end{bmatrix}, \mathbf{B}_1 = \begin{bmatrix} -28.769 & 0 \\ 0 & 1 \\ 50.229 & 0 \end{bmatrix}, \mathbf{B}_2 = \begin{bmatrix} 318.7 \\ 0 \\ -202.2 \end{bmatrix}.$$

Using the technique presented in Theorem 1 and solving (13) via Matlab LMI toolbox [54], the H_∞ controller is obtained as:

$$u = [0.1627 \qquad 4.5475 \qquad 0.7761]\,\mathbf{x}, \tag{15}$$

with H_∞ gain $\gamma = 4.9139$.

Velocity measurements are not available from experiments. In [55], the authors propose a controller modification to overcome the lack on velocities measurements. So, the velocity part is replaced by a first-order linear compensator [55]:

$$\begin{aligned} u &= 0.3\,(0.1627\,\dot{p}_1 + 4.5475\,\theta_2 + 0.7761\,\dot{p}_2)\,, \\ \dot{p}_1 &= -10p_1 + 5\theta_1, \\ \dot{p}_2 &= -10p_2 + 5\theta_2. \end{aligned} \tag{16}$$

The controller in (16) is multiplied by 0.3 to compensate internal gains. The terms p_1 and p_2 are auxiliary variables and their differential equations are solved numerically from θ_1 and θ_2 measurements. The above equations are a direct implementation of controller modification given in [55], where the parameter -10 is set according to [56] and the gain 5 is adjusted experimentally.

Remark 1. *By taking into account that the separation principle is commonly invoked to design an observer separated from plant dynamics, our controller scheme (16) was then designed by following this principle (see [56] and [57]).*

The load disk movement is controlled by the robust control law (15) implemented on the computer. This law tries to stabilize the inverted pendulum despite the external disturbance, by moving the load disk. So, some kind of navigation is obtained, because this perturbation is induced externally through the MDC device (see Figure 7). Figures 8-10 show the load and pendulum displacement, and the control effort. Notice from Figure 8 that a very small pendulum displacement (less than 1 deg.) induces a navigation on the load disk (see Figure 9). This pendulum displacement comes from the external disturbance. Also, a video is uploaded with the main paper, to show the experiment development and

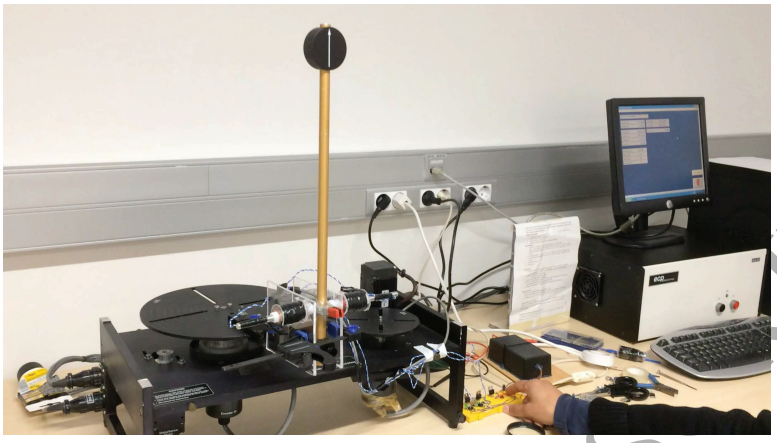

Figure 7: The load disk movement is induced externally, through a perturbation produced by the electromagnetic device. So, the pendulum is maintained on its upload position and base disk moves left and right due to this commanded disturbance (see video https://youtu.be/81H_xmApoes).

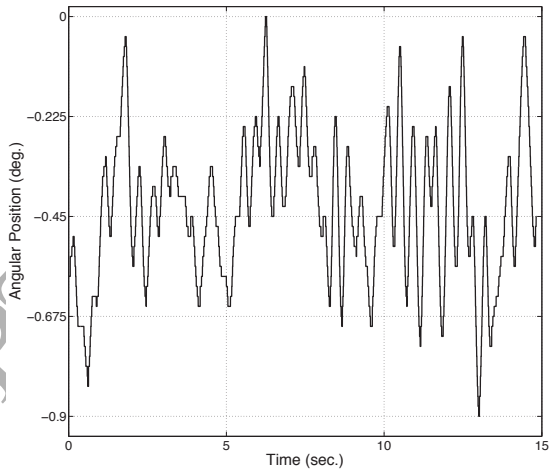

Figure 8: Pendulum position. The initial position is set manually, so a little error is introduced, and the pendulum is not centered exactly on zero angular position (non-stable position).

205 confirm the objective of this paper: the designed control stabilizes the inverted pendulum, using the MDC device to create an external perturbation. The video

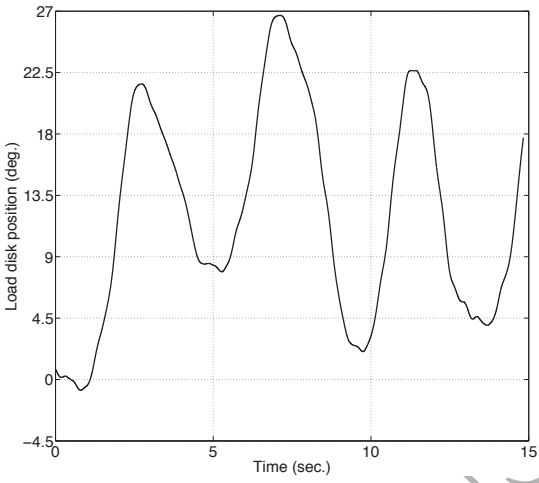

Figure 9: Load disk position. The displacement is over 25 degrees. The initial position is set manually, so a little error is introduced.

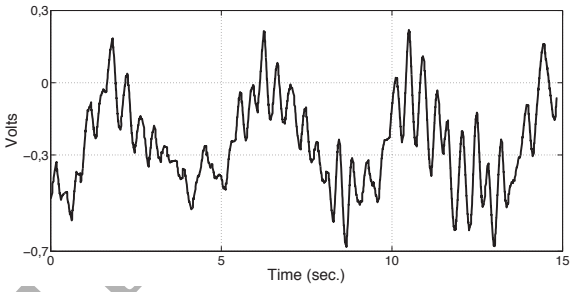

Figure 10: Control effort. The control is reseted before the experiment, but due to the manually set initial position, an initial effort is introduced.

of this experiment can be seen at https://youtu.be/81H_xmApoes.

5.3. Disturbance observer

As said previously, the main motivation of this paper is to emulate the navigation of a sub-actuated mechanism without touching it. To evince this affirmation, we consider now a disturbance observer. Then, a study on how the MDC disturbances induce navigation on the load disk is experimentally validated. A

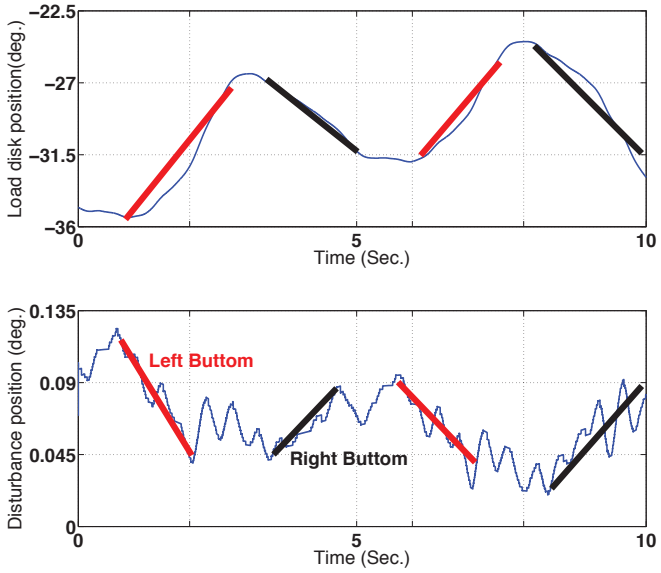

Figure 11: Disturbance observer versus load position (first 10sec). MDC: the right push-button 'moves' the load disk in clockwise; the left one in counter-clock wise. The MDC push-buttons are activated by pulses. Small delay can be appreciated.

comparison between the displacement of the load disk and the observed disturbance is done. Moreover, we can appreciate that MDC's left/right push-button induces movement on the load disk. Fig. 11 pictures the load position compared to the observed disturbance, showing the navigation of the system. In [58], a survey of disturbance observer can be found. Here, we consider an state based on observer. From (10), we obtain

$$\mathbf{B_1}\omega = \dot{\mathbf{x}} - \mathbf{A}\mathbf{x} - \mathbf{B_2}u.$$

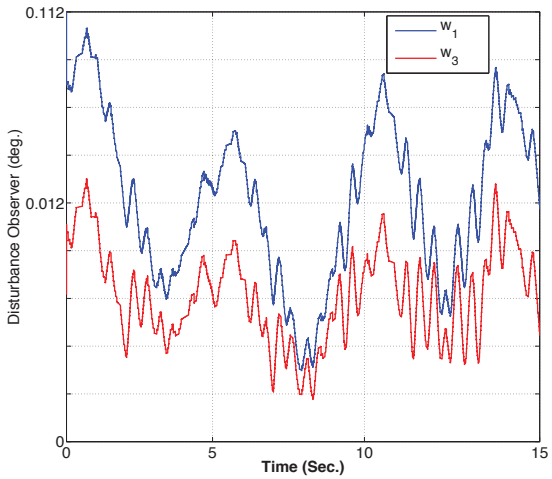

Figure 12: The disturbance is registered by using (17). Notice that $\hat{w}_1$ and $\hat{w}_3$ have a similar behavior. The external perturbation can be an average of these two signals.

Considering the notation $A = (A(i,j))$, $B_1 = (B_1(i,1))$, and $B_2 = (B_2(i,1))$, for $i,j \in \{1,2,3\}$, we obtain

$$\begin{bmatrix} B_1(1,1)w \\ \dot{w} \\ B_1(3,1)w \end{bmatrix} = \begin{bmatrix} \dot{x}_1 \\ \dot{x}_2 \\ \dot{x}_3 \end{bmatrix} - \begin{bmatrix} A(1,1) & A(1,2) & 0 \\ 0 & 0 & 1 \\ A(3,1) & A(3,2) & 0 \end{bmatrix} \begin{bmatrix} x_1 \\ x_2 \\ x_3 \end{bmatrix} - \begin{bmatrix} B_2(1,1) \\ 0 \\ B_2(3,1) \end{bmatrix}.$$

Following the idea presented in [59], consider $\hat{w}_1$ as the perturbation observed from $\dot{x}_1$, $\hat{\dot{w}}$ as the velocity of the perturbation appreciated from $\dot{x}_2$, and $\hat{w}_3$ as the perturbation noted from $\dot{x}_3$. Then, we define the observer as:

$$\begin{aligned} \hat{w}_1 &= \tfrac{1}{B_1(1,1)}\left(\dot{x}_1 - A(1,1)x_1 - A(1,2)x_2 - B_2(1,1)u\right) \\ \hat{\dot{w}} &= \dot{x}_2 - x_3 \\ \hat{w}_3 &= \tfrac{1}{B_1(3,1)}\left(\dot{x}_3 - A(3,1)x_1 - A(3,2)x_2 - B_2(3,1)u\right). \end{aligned} \tag{17}$$

From experiments, we obtain $\hat{w}_1 \simeq \hat{w}_3$ (Fig. 12) and $\hat{\dot{w}} \simeq 0$ (Fig. 13).

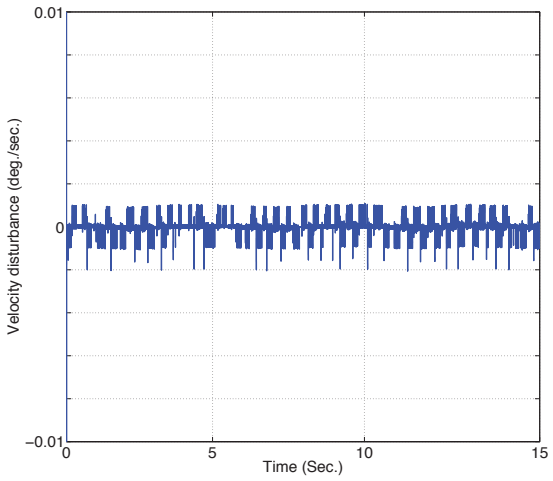

Figure 13: Observed velocity of the external disturbance. The calculated velocity $\hat{w}$ is almost zero.

6. Conclusions

The main motivation of work was to design a new experimental platform to test user navigation command via external induced magnetic disturbance forces and applied to a class of under-actuated systems. A way to perform this objective is to implement a stabilizer in front of disturbances, following a well-tuned control objective, in order to interpret the perturbation as an user command.

That is, we have designed magnetic driving commands (MDC) to create a tiny disturbance on the inverted pendulum, without contact. The controller stabilizes the inverted pendulum by rotating the load disk, inducing navigation on the system. The control problem is solved via the well-known H_∞ theory, using classical LMI technique. The proposed linear feedback controller is then robust against external perturbations and model uncertainties. The MDC device has been implemented with electromagnetic coils connected to two switches, allowing clockwise and counter-clock wise displacements. Experiments are carried out to show the effectiveness of our approach. Moreover, to highlight the nov-

elty of the contribution, a disturbance observer is designed to experimentally validate the main contribution and control objective.

7. Furute work

The extension of the LMI-based controller design based on velocity observer for this system with disturbances and multiple time-varying delays will be presented in the future work. Also, it can be interesting to extend this work to regional pole constraints procedure, allowing to move the chosen poles to a pre-specified region of the complex plane.

8. Acknowledgment

This work was partially supported by the Spanish Ministry of Economy, Industry and Competitiveness, under grants DPI2016-77407-P (AEI/FEDER, UE) and DPI2015-64170-R (MINECO/FEDER). Also, we want to express our sincere gratitude to the reviewers for their useful and constructive comments.

9. Appendix

9.1. Friction at the pendulum

Consider the Coulomb friction applied to the pendulum equation (7), with coefficient c_2:

$$\ddot{\theta}_1 m R_h l_{cg} \cos(\theta_2) + \ddot{\theta}_2 \bar{J}_z - \tfrac{1}{2}\dot{\theta}_1^2(\bar{J}_x - J_y)\sin(2\theta_2) - mgl_{cg}\sin(\theta_2) +$$

$$+ mR_h \sin(\theta_2)\dot{\theta}_1 - \dot{\theta}_1\dot{\theta}_2 m R_h l_{cg}\sin(\theta_2) = -c_2 \mathrm{sign}(\dot{\theta_2}),$$

The value of c_2 is unknown but small compared to the other system parameters. Then, the friction on the mechanical pendulum system can be neglected. If friction is considerable, it can be viewed as an additive perturbation on the system, and compensated with the robust control design.

9.2. Proof of Theorem 1

Proof of Theorem 1 is now presented. First, Projection lemma and Schur complements are stated:

Lemma 1 (Projection lemma [43, 53]). *For a symmetric matrix Ψ and matrices $\mathbf{P}$ and $\mathbf{S}$ with appropriate dimensions, there exists a matrix $\mathbf{X}$ such that:*

$$\Psi + \mathbf{P}^T\mathbf{X}^T\mathbf{S} + \mathbf{S}^T\mathbf{X}\mathbf{P} < 0 \Leftrightarrow \begin{cases} \mathcal{N}_P^T \Psi \mathcal{N}_\mathbf{P} < 0 \\ \\ \mathcal{N}_\mathbf{S}^T \Psi \mathcal{N}_\mathbf{S} < 0 \end{cases}$$

with $\mathcal{N}_\mathbf{P}$ and $\mathcal{N}_\mathbf{S}$ any matrices whose columns form bases of $\mathbf{P}$ and $\mathbf{S}$, respectively.

Lemma 2 (Schur Complements [52]). *Consider a symmetric matrix $\mathbf{M} = \begin{pmatrix} \mathbf{P}_1 & \mathbf{P}_2 \\ \mathbf{P}_2^T & \mathbf{P}_3 \end{pmatrix}$. Then, $\mathbf{M} < 0$ if and only if $\mathbf{P}_1 - \mathbf{P}_2\mathbf{P}_3^{-1}\mathbf{P}_2^T < 0$ and $\mathbf{P}_3 < 0$ is invertible.*

Proof of Theorem 1. Consider the Lyapunov function $V(\mathbf{x}) = \mathbf{x}^T\mathbf{X}\mathbf{x}$, with symmetric matrix $\mathbf{P} > 0$. From (12), one can obtain:

$$(\mathbf{A}\mathbf{x} + \mathbf{B}_2 u + \mathbf{B}_1\omega)^T\mathbf{X}x + (*) + \gamma^{-1}(\mathbf{C}_1\mathbf{x} + \mathbf{D}_{12}u)^T(\mathbf{C}_1\mathbf{x} + \mathbf{D}_{12}u) - \gamma\omega^T\omega < 0.$$

System matrices $\mathbf{C_1}$ and $\mathbf{D_{12}}$ verify the H_∞ assumption [42]: $\mathbf{D}_{12}^T[\mathbf{C}_1 \quad \mathbf{D}_{12}] = [0\ I]$. Considering $\mathbf{v}^T = (\mathbf{x}^T, \omega^T)$, this inequality can be re-written as

$$v^T \begin{bmatrix} \Omega & * \\ \\ \mathbf{B}_1^T\mathbf{X} & -\gamma \end{bmatrix} v < 0\,, \tag{18}$$

with

$$\Omega := (\mathbf{A} + \mathbf{B}_2\mathbf{K})^T\mathbf{X} + (*) + \gamma^{-1}\mathbf{C}_1^T\mathbf{C}_1 + \gamma^{-1}\mathbf{K}^T\mathbf{K}\,.$$

First, the Schur complement is applied to (18) as a first step to linearize it:

$$\begin{bmatrix} (\mathbf{A}+\mathbf{B}_2\mathbf{K})^T\mathbf{X}+(*) & * & * & * \\ \mathbf{B}_1^T\mathbf{X} & -\gamma & * & * \\ \mathbf{C}_1 & 0 & -\gamma & * \\ \mathbf{K} & 0 & 0 & -\gamma \end{bmatrix} < 0\,, \tag{19}$$

The proof goes through applying the Projection Lemma. Consider $\mathbf{N} := \mathbf{KV}$, $\mathbf{P} := (\mathbf{I}, 0, 0, 0, 0, 0)$, $\mathbf{S} := (-\mathbf{I},\ (\mathbf{A}+\mathbf{B}_2\mathbf{K})^T,\ 0,\ \mathbf{C}_1^T, \mathbf{K}^T,\ \mathbf{I})$ and

$$\Psi := \begin{pmatrix} 0 & * & * & * & * & * \\ \mathbf{Y} & -\mathbf{Y} & * & * & * & * \\ 0 & \mathbf{B}_1^T & -\gamma & * & * & * \\ 0 & 0 & 0 & -\gamma & * & * \\ 0 & 0 & 0 & 0 & -\gamma & * \\ 0 & 0 & 0 & 0 & 0 & -Y \end{pmatrix}.$$

Thus, we re-write (13) as $\Psi + \mathbf{P}^T\mathbf{V}^T\mathbf{S} + \mathbf{S}^T\mathbf{V}\mathbf{P} < 0$. Now, by the Projection Lemma, if (13) is feasible, the inequality $\mathcal{N}_\mathbf{S}^T\psi\mathcal{N}_\mathbf{S} < 0$ holds. The null spaces bases of S is

$$\mathcal{N}_\mathbf{S} = \begin{pmatrix} (\mathbf{A}+\mathbf{B}_2\mathbf{K})^T & 0 & \mathbf{C}_1^T & \mathbf{K}^T & \mathbf{I} \\ \mathbf{I} & 0 & 0 & 0 & 0 \\ 0 & \mathbf{I} & 0 & 0 & 0 \\ 0 & 0 & \mathbf{I} & 0 & 0 \\ 0 & 0 & 0 & \mathbf{I} & 0 \\ 0 & 0 & 0 & & \mathbf{I} \end{pmatrix}.$$

From $\mathcal{N}_\mathbf{S}^T\psi\mathcal{N}_\mathbf{S} < 0$, we have

$$\begin{pmatrix} (\mathbf{A}+\mathbf{B}_2\mathbf{K})\mathbf{Y}+\mathbf{Y}(\mathbf{A}+\mathbf{B}_2\mathbf{K})^T-\mathbf{Y} & * & * & * & * \\ \mathbf{B}_1^T & -\gamma & * & * & * \\ \mathbf{C}_1^T\mathbf{Y}^T & 0 & -\gamma & * & * \\ \mathbf{K}^T\mathbf{Y}^T & 0 & 0 & -\gamma & * \\ \mathbf{Y}^T & 0 & 0 & 0 & -\mathbf{Y} \end{pmatrix} < 0\,. \tag{20}$$

Consider $\mathbf{Q} = diag(-\gamma, -\gamma, -\gamma)$. Applying Schur complement on (20), we obtain

$$(\mathbf{A}+\mathbf{B}_2\mathbf{K})\mathbf{Y}^T + \mathbf{Y}(\mathbf{A}+\mathbf{B}_2\mathbf{K})^T - (\mathbf{B}_1 \quad \mathbf{Y}\mathbf{C}_1^T \quad \mathbf{Y}\mathbf{K}^T)\mathbf{Q}^{-1}\begin{pmatrix} \mathbf{B}_1 \\ \mathbf{C}_1\mathbf{Y}^T \\ \mathbf{K}\mathbf{Y}^T \end{pmatrix} < 0 .$$

Using $\mathbf{Y} = \mathbf{X}^{-1}$, and applying again Schur complement, it is easy to see that equation (19) is obtained. Then, condition (12) is verified and $u = \mathbf{N}\mathbf{V}^{-1}\mathbf{x}$ is an H_∞ controller. □

References

References

[1] B.S. Cazzolato, Z. Prime, On the Dynamics of the Furuta Pendulum, J. of Contr. Sc. and Eng., (2011) 1–8, doi:10.1155/2011/528341.

[2] K.L. Astrom, K. Furuta, Swinging up a pendulum by energy control, Automatica, 36 (2000) 287-295.

[3] S. Awtar, N. King, T. Allen, I. Bang, M. Hagan, D. Skidmore, K. Graig, Inverted pendulum systems: rotary and arm-driven- a mechatronic system design case study, Mechaton., 12 (2002) 357–370.

[4] Y. Xu, H.-Y. Shum, Dynamic control and coupling of a free-flying space robot system, J. of Robotic Syst., 11(7) (1994) 573–589, doi: 10.1002/rob.4620110702

[5] G. Antonelli, Underwater Robots: Motion and Force Control of Vehicle- Manipulator Systems, Springer Tracts in Advanced Robotics Springer-Verlag Inc., New York 2006.

[6] S.K. Dwivedy, P. Eberhard, Dynamic analysis of flexible manipulators, a literature review, Mechanism and Machine Theo., 41(7) (2006) 749–777, doi:10.1016/j.mechmachtheory.2006.01.014

[7] S. Mobayen, D. Baleanu, F. Tchier, Second-order fast terminal sliding mode control design based on LMI for a class of non-linear uncertain systems and its application to chaotic systems, J. of Vibration and Contr., 23(18) (2017) 2912–2925, doi:10.1177/1077546315623887

[8] S. Mobayen, Design of LMI-based sliding mode controller with an exponential policy for a class of under-actuated systems, Complexity 21(5) (2016) 117–124.

[9] N. Sun, Y. Wu, Y. Fang, H. Chen, B. Lu, Nonlinear Continuous Global Stabilization Control for Underactuated RTAC Systems: Design, Analysis, and Experimentation, IEEE/ASME Transa. on Mech. 22(2) (2017) 1104–1115, Doi: 10.1109/TMECH.2016.2631550

[10] X. Huang, Ye. Yan, Saturated Backstepping Control of Underactuated Spacecraft Hovering for Formation Flights, IEEE Trans. on Aerospace and Electr. Syst. 53(4) (2017) 1988–2000.

[11] D.Pucci, S. Traversaro, F. Nori, Momentum Control of an Underactuated Flying Humanoid Robot, IEEE Robot. and Aut. Lett., 3(1) (2018) 195–202.

[12] Y. Orlov, L. Aguilar, L. Acho, Zeno mode control of underactuated mechanical systems with application to the Pendubot stabilization around the upright position, Proc. 16th IFAC World Congress (2005).

[13] J. Warminski, S. Lenci, M.P. Cartmell, G. Rega, M. Wiercigroch, Nonlinear Dynamic Phenomena in Mechanics (Section 4.2), (2011) Springer Science and Business Media.

[14] H.G. Nguyen, J. Morrell, K. Mullens, A. Burmeister, S. Miles, N. Farrington, K. Thomas, D.W. Gagee. Segway robotic mobility platform. SPIE Proceedings 5609: Mobile Robots XVII, Philadelphia, PA, October 27-28, 2004.

[15] T. Horibe, N. Sakamoto. Optimal swing up and stabilization control for inverted pendulum via stable manifold method. IEEE Trans. on Contr. Syst. Tech., 26(2) (2018) 708–715.

[16] K. Yokoyama, M. Takahashi, Dynamics-Based Nonlinear Acceleration Control With Energy Shaping for a Mobile Inverted Pendulum With a Slider Mechanism, IEEE Trans. on Contr. Syst. Tech., 24(1) (2016) 40–55.

[17] I. Hassanzadeh, S. Mobayen, A. Harifi, Input-Output Feedback Linearization Cascade Controller Using Genetic Algorithm for Rotary Inverted Pendulum System, American J. of Appl. Sciences, 5(10) (2008) 1322–1328.

[18] P. Dwivedi, S. Pandey, A.S. Junghare. Stabilization of unstable equilibrium point of rotary inverted pendulum using fractional controller, J. of the Franklin Inst., 354 (2017) 7732–7766.

[19] Y.-H. Li, G.-Z. Cao, S.-X. Tang, X.-S. Cai, J.-Z. Peng. Energy-based stabilization and H_∞ robust stabilisation of stochastic non-linear systems, IET contr. The. and Appl., 12(2) (2017) 318–325.

[20] L. Messikh, El.H. Guechi, M.L. Benloucif, Critically damped stabilization of inverted-pendulum systems using continuous-time cascade linear model predictive control, J. of the Franklin Inst., 354 (2017) 7241–7265.

[21] S. Ri, J. Huang, Y. Wang, M. Kim, S. An, Terminal sliding mode control of mobile wheeled inverted pendulum system with nonlinear disturbance observer, Math. Probl. in Eng. (2014) 1–8, doi: 10.1155/2014/284216.

[22] Z.-Q. Guo, J.-X. Xu, T.H. Lee, Design and implementation of a new sliding mode controller on an underactuated wheeled inverted pendulum, Journal of the Franklin Institute, 351(4) (2014) 2261-2282.

[23] M. Muehlebach, R. DAndrea, Nonlinear Analysis and Control of a Reaction-Wheel-Based 3-D Inverted Pendulum, IEEE Trans. on Contr. Syst. Tech., 25(1) (2017) 235–246, DOI: 10.1109/TCST.2016.2549266.

[24] I. Hassanzadeh, S. Mobayen, Controller Design for Rotary Inverted Pendulum System Using Evolutionary Algorithms, Mathematical Problems in Engineering, (2011) 1-17.

[25] H. Hoang, M. Wongsaisuwan, Robust Controller Design for a Rotary Double Inverted Pendulum using Linear Matrix Inequalities, Conf. of the Soc. of Instr. and Contr. Eng. (2007) 515–520.

[26] V.M. Hernández-Guzmán, M. Anatonio-Cruz, R. Silva-Ortigoza, Linear State Feedback Regulation of a Furuta Pendulum: Design Based on Differential Flatness and Root Locus, IEEE Access, 4 (2016) 8721–8736, doi:10.1109/ACCESS.2016.2637822.

[27] H. Gritli, S. Belghith, Robust feedback control of the underactuated Inertia Wheel Inverted Pendulum under parametric uncertainties and subject to external disturbances: LMI formulation, J. of the Franklin Inst., (2017), doi:10.1016/j.jfranklin.2017.01.035.

[28] W. Ye, Z. Li, C. Yang, J. Sun, C-Y. Su, R. Lu, Vision-Based Human Tracking Control of a Wheeled Inverted Pendulum Robot, IEEE Trans. on Cyber. 46(11) (2016) 2423–2434, doi: 10.1109/TCYB.2015.2478154.

[29] S. Mobayen, An LMI-based robust tracker for uncertain linear systems with multiple time-varying delays using optimal composite nonlinear feedback technique, Nonlinear Dyn., 80:917 (2015) doi:10.1007/s11071-015-1916-5.

[30] C. Aguilar-Avelar, J. Moreno-Valenzuela, A composite controller for trajectory tracking applied to the Furuta pendulum, ISA Trans. 57 (2015) 286–294.

[31] F. Bayat, S. Mobayen, S. Javadi, Finite-time tracking control of n^{th}-order chained-form non-holonomic systems in the presence of disturbances, ISA Trans. 63 (2016) 78–83.

[32] S. Mobayen, S. Javadi, Disturbance observer and finite-time tracker design of disturbed third-order nonholonomic systems using terminal sliding mode. J. of Vibr. and Contr. 23(2) (2017) 181–189.

[33] W. Ye, Z. Li,C. Yang, J. Sun, C.-Y. Su, R. Lu, Vision-Based Human Tracking Control of a Wheeled Inverted Pendulum Robot, IEEE Trans. on Cybern., 46(11) (2016) 2423–2434, doi: 10.1109/TCYB.2015.2478154.

[34] M.Yue, S. Wang, J.-Z. Sun, Simultaneous balancing and trajectory tracking control for two-wheeled inverted pendulum vehicles: A composite control approach, Neurocomputing 191 (2016) 4454, http://dx.doi.org/10.1016/j.neucom.2016.01.008.

[35] B. Srinivasan, P. Huguenin, D. Bonvin, Global stabilization of an inverted pendulum - Control strategy and experimental verification, Automatica 45(1) (2009) 265–269.

[36] S. Sun, S. Ionita, E. Volná, A. Gavrilov, F. Liu, PD control of inverted pendulum based on adaptive fuzzy compensation, J. of Intell. and Fuzzy Syst., 31(6) (2016) 3013-3019, doi: 10.3233/JIFS-169186.

[37] S. Jung, J.K. Ahn, Remote Control of an Inverted Pendulum System for Intelligent Control Education, Systemics, Cyber. and Inform., 9(4) (2011) 49–54

[38] M. Sowmiya, R. Thenmozhi, Navigation of Mobile Inverted Pendulum via Wireless control using LQR Technique, Inter. J. for Modern Trends in Science and Tech., 2(06) (2016) 92–97.

[39] L. Wei, Y. Shen, M. Jiang, Q. Chen, M. Fei, A Platform Based on Inverted Pendulum for NCSs, Proc. of the 8th W. Cong. on Intelligent Contr. and Automation, (2010) 4386–4389, Jinan, China.

[40] T. Shinbrot, C. Grebogi, E. Ott, J.A. Yorke, Using small perturbations to control chaos, Nature, 363 (1993), 411–417.

[41] Y. Zhou, C.K. Tse, S.-S. Qiu, F.C.M. Lau, Applying resonant parametric perturbation to control chaos in the buck dc/dc converter with phase shift and frequency mismatch considerations, Intern. J. of Bifurc. and Chaos, 13(11) (2003) 34593471.

[42] J.C. Doyle, K. Glover, P.P. Khargonekar, B. A. Francis, State-space solutions to standard H_2 and $_\infty$ control problems, IEEE Trans. on Aut. Contr., 34(8) (1989) 831–847.

[43] P. Gahinet, P. Apkarian, A linear matrix inequality approach to H_∞ control, Inter. J. of Nonlinear Control, 4 (1994) 421–448.

[44] P. Khargonekar, I. Petersen, K. Zhou, Robust stabilization of uncertain linear systems: quadratic stabilization and H_∞ control theory, IEEE Tran. on Aut. Control, 35(3) (1990) 356–361.

[45] S. Boyd, L. El Ghaou, E. Feron, V. Balakrishnan, Linear Matrix Inequalities in System and Control Theory, SIAM, Philadelphia, USA,1994.

[46] ECP Model. Manual for A-51 inverted pendulum accessory (Model 220), Educational Control Products, California 91307, USA, 2003.

[47] G. Pujol, L. Acho, Stabilization of the Furuta pendulum with backlash using H_∞-LMI technique: Experimental validation, Asian Journal of Control, 12(4) (2010) 460–467.

[48] H.D. Tuan, P. Apkarian, T.Q. Nguyen, Robust Filtering for Uncertain Nonlinearly Parameterized Plants,IEEE Trans. on Signal Process., 51(7) (2003) 1816–1824.

[49] H. Yang, Y. Xia1,P. Shi, Stabilization of networked control systems with nonuniform random sampling periods, Int. J. Robust. Nonlinear Control, 21 (2011) 501–526.

[50] H. Azizan, M. Jafarinasab, S. Behbahani, M.Danesh, Fuzzy Control Based on LMI Approach and Fuzzy Interpretation of the Rider Input For Two Wheeled Balancing Human Transporter, 8th IEEE Int. Conf. on Contr. and Aut., China, 2010.

[51] C. Olalla, R. Leyva, A. El Aroudi, P. Garcs, I. Queinnec, LMI robust control design for boost PWM converters, IET Power Electron., 3(1) (2010) 75–85, doi: 10.1049/iet-pel.2008.0271.

[52] P. Apkarian, H.D. Tuan, J. Bernussou, Continuos-Time analysis, eigenstructure assignment and H_2 synthesis with enhanced LMI characterizations, IEEE Trans. on Automatic Contr., 46(12) (2001) 1941–1946.

[53] G. Pujol, J. Rodellar, J.-M. Rossell, Reliable control for parametrized interconnected systems using LMI techniques, Proc. of IFAC conf. (2005) 1–6, Prague, Chec. Republic.

[54] R.Y. Chiang and M.G. Safonov, Matlab Robust Control Toolbox User's Guide version 2, The MathWorks Inc., MA, USA, 1998.

[55] H. Berghuis, H. Nijmeijer , Global regulation of robots using only position measurements, Syst. and Control Lett. 21(1993) 289–293.

[56] K. Ogata, Modern control engineering (Chapter 12), Prentice-Hall, New York, 1997.

[57] H.K. Khalil., Nonlinear systems, Prentice-Hall, New York, 2000.

[58] W.-H. Chen, J. Yang, L. Guo, S. Li, Disturbance-observer-based control and related methods-An overview, IEEE Trans. on Industr. Electron. 63(2) (2016) 1083–1095.

[59] C. Milosavljevic, B. Veselic, D. Mitic, Discrete-time quasi-sliding mode control systems - Part II, Electronics 9(2) (2005).